ELSEVIER

Quaternary Science Reviews 26 (2007) 829–835

QSR
RAPID COMMUNICATION

Rapid communication

Variable ^{10}Be fluxes in lacustrine sediments from Tristan da Cunha, South Atlantic: a solar record?

Karl Ljung[a,*], Svante Björck[a], Raimund Muscheler[a,b], Jürg Beer[c], Peter W. Kubik[d]

[a]*GeoBiosphere Science Centre, Quaternary Sciences, Lund University, Sölveg. 12, SE-223 62 Lund, Sweden*
[b]*NASA/Goddard Space Flight Center, Climate & Radiation Branch, Mail Code 613.2, Greenbelt, MD 20771, USA*
[c]*EAWAG, Ueberlandstrasse 133, Postfach 611, CH-8600 Duebendorf, Switzerland*
[d]*Paul Scherrer Institut c/o Institute of Particle Physics, HPK H30, ETH Hoenggerberg, CH-8093 Zurich, Switzerland*

Received 19 July 2006; received in revised form 15 December 2006; accepted 30 December 2006

Abstract

A 650-yr-long sediment sequence from a crater lake on Tristan da Cunha, South Atlantic, was analysed for its ^{10}Be content. Based on ^{14}C dating, and sedimentary, geochemical, magnetic and palynological records, the period between 900 and 1450 AD appears to have been unusually stable in terms of sedimentation and vegetation and therefore this period was chosen for analysis of the ^{10}Be content. During this period of highly organic sedimentation and closed vegetation, the pattern of ^{10}Be flux variations follows the ^{10}Be fluctuations from the GRIP ice core and estimated ^{14}C production rates well. However, before and after this stable period, variable sedimentation rates have to be accounted for to obtain results that are comparable to the established ^{10}Be/^{14}C records. Our data show not only the possibility of obtaining detailed enough ^{10}Be flux data from sedimentary sequences to reconstruct past solar forcing but also how sensitive this type of record is to sedimentary and environmental changes. If suitable archives can be found, they have the potential to improve reconstructions of solar activity far back in time.

1. Introduction

The production rates of cosmogenic radionuclides in the Earth's atmosphere are influenced by the geo- and heliomagnetic shielding of galactic cosmic rays (Lal and Peters, 1967). Strong solar magnetic fields ejected from the Sun into the heliosphere and high geomagnetic field intensities cause a stronger deflection of the galactic cosmic rays that produce cosmogenic radionuclides such as ^{10}Be and ^{14}C. The physical mechanisms behind the production processes are well understood, which make radionuclide records reliable recorders of the history of the solar magnetic activity (Lal and Peters, 1967; Masarik and Beer, 1999). The geochemical behaviour of cosmogenic radionuclides after their production introduces uncertainties in interpreting these records. Radiocarbon, for example, forms CO_2 and enters the complex carbon cycle (Siegenthaler et al., 1980), while in the case of ^{10}Be the climatic influence on atmospheric transport and deposition introduces uncertainties in obtaining the solar-induced production signal. So far, only polar ice core records have provided reliable data that allowed the reconstruction of past solar activity changes. ^{10}Be measurements in lake sediments are usually more complicated to interpret since potential climate influences are more likely to dominate the signal (Houriuchi et al., 1999). In addition, for solar activity reconstructions high temporal resolution is required. Besides the well-known 11-yr cycle, typical solar variations act on time scales of centuries with, e.g., the Maunder minimum as one example (e.g., Beer et al., 1990). Ice core records are generally restricted to high latitudes, therefore independent ^{10}Be records from lower latitudes can improve the estimates about past solar forcing, since polar records might be biased due to the absence of the geomagnetic shielding of galactic cosmic rays at high latitudes (Field et al., 2006).

The radiocarbon method (Libby, 1955) is commonly used to date sediments for obtaining a chronology on, e.g. climate proxy records, but an even more accurate dating

*Corresponding author. Tel.: +464622278888; fax: +4646397010.
E-mail address: karl.ljung@geol.lu.se (K. Ljung).

0277-3791/$ - see front matter © 2007 Elsevier Ltd. All rights reserved.
doi:10.1016/j.quascirev.2006.12.016

can be achieved by high-resolution measurements of both ^{14}C and ^{10}Be. If periods of increased or reduced ^{14}C and ^{10}Be production rates can be identified and matched in different natural archives, very accurate datings and correlations between different climate records could be obtained (Van Geel and Mook, 1989). In addition to study leads and lags in climate change with respect to the influence of solar forcing, the apparently best situation is to identify the solar forcing and the climate response in the same sediment sequence.

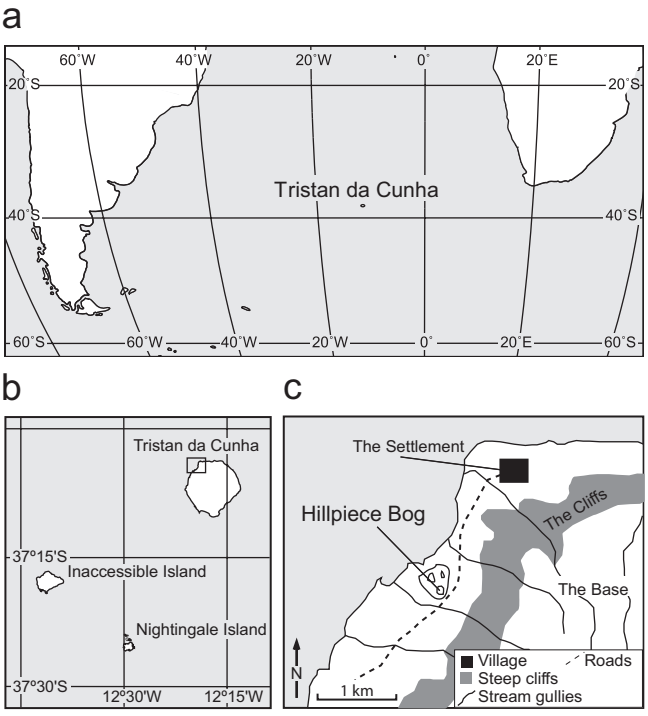

Fig. 1. The position of the island of Tristan da Cunha in the middle of the South Atlantic (upper), with its position in relation to the other islands of the Tristan da Cunha Island Group (down left), and location of the Hillpiece Bog in relation to other geographic features. The peak of Tristan da Cunha reaches 2060 m above sea level.

2. Background

As a result of an expedition to Tristan da Cunha (Fig. 1), highly organic, unique lacustrine sediments were found in one of the cored volcanic crater lakes, the Hillpiece Bog (37° 05′S, 12° 17′W) (Ljung et al., 2006). The environmental history of the site has been studied with a multiproxy approach and is presented in Ljung et al. (2006). The bog is situated at 62 m above sea level, and is only 220 m^2 in size, surrounded by gently sloping crater walls and with a catchment size of ca 4500 m^2. The chronology of the sediment sequence was determined by 12 radiocarbon dates on terrestrial macrofossils and bulk sediment (Ljung et al., 2006). Six of these dates are within the section presented here (Table 1). During the lake phase and before humans opened up the landscape, the site was a small pond surrounded by very dense vegetation (Ljung et al., 2006). With the exception of one thin tephra layer, the sediments formed between 600 and 1600 AD contain 40–50% total organic carbon (TOC), i.e. almost pure organic matter. Furthermore, the sediments formed between 950 and 1400 AD are very homogenous and show no changes in sedimentation rate or lithology (Fig. 2), and mainly consist of fine-grained organic particles and also some clay, with the ^{10}Be being attached to both (McHargue and Damon, 1991). The almost pure organic matter shows that the lake was highly productive, and that any surface run-off mainly brought organic material into the lake with constant deposition rate between 950 and 1400 AD. During this period, the uniform pollen composition showed very stable vegetation (Fig. 2). In addition, the surrounding volcanic bedrock is barren of ^{10}Be (Baker et al., 1964), and the high precipitation ($>1500\,mm\,yr^{-1}$) generates short transport times from the small catchment to the lake. These conditions are good prerequisites to avoid potential problems with variable ^{10}Be fluxes (cf Anderson et al., 1990; Chase et al., 2002) often related to variable surface run-off conditions, thereby changing the chemistry and grain size of the sediments. However, most reports on scavenging and sedimentary effects on ^{10}Be fluxes come from the marine environment (Frank et al., 1997; Christl et al., 2003).

Table 1
Radiocarbon dates from Hillpiece Bog

Lab nr.	Depth (cm)	^{14}C yr BP	Cal yr BP, 1σ	Cal yr BP, 2σ	Material
LuS-6303	181–182	240 ± 50	310BP (24.6%) 260BP 230BP (43.6%) 140BP	440BP (2.5%) 400BP 330BP (92.9%) −11BP	Twigs, seeds, leaves
Poz-3422	194.0–194.5	480 ± 30	520BP (68.2%) 485BP	535BP (95.4%) 450BP	*Phylica* leaves, twigs
Poz-3423	222–223	820 ± 30	725BP (68.2%) 675BP	740BP (95.4%) 665BP	*Phylica* leaves, twigs
Poz-3224	253.0–253.5	1085 ± 30	965BP (68.2%) 925BP	1060BP (4.0%) 1030BP 990BP (89.5%) 900BP 870BP (1.9%) 840BP	*Phylica* leaves, twigs
Poz-3425	293–294	1295 ± 35	1260BP (32.5%) 1200BP 1190BP (28.0%) 1130BP 1110BP (7.7%) 1090BP	1270BP (95.4%) 1070BP	*Phylica* leaves, twigs
Poz-3426	308.0–308.5	1475 ± 25	1340BP (68.2%) 1295BP	1370BP (95.4%) 1285BP	*Phylica* leaves, twigs
Poz-3427	345–344	1790 ± 30	1700BP (65.5%) 1600BP 1580BP (2.7%) 1570BP	1720BP (95.4%) 1540BP	*Phylica* leaves, twigs

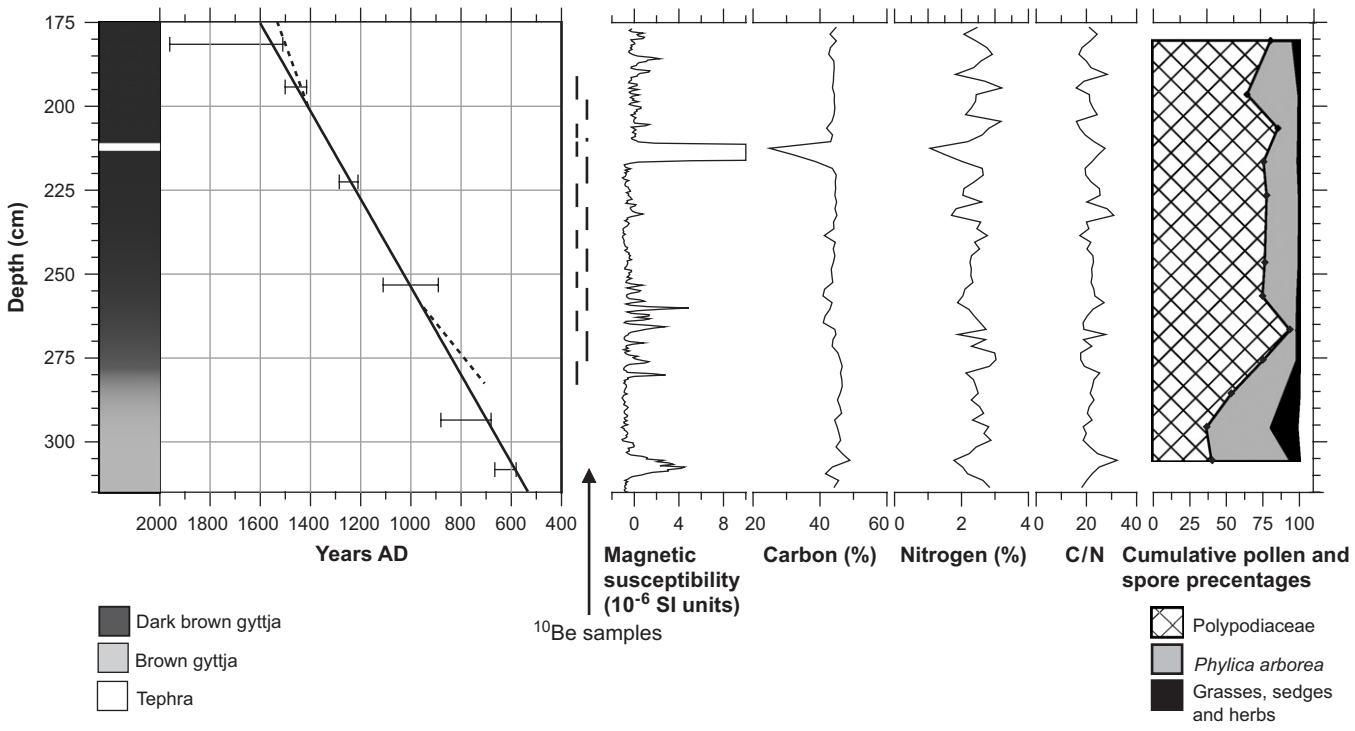

Fig. 2. A composite diagram of the age-depth function with some proxy records. Shown from left to right: sediment depth, lithology, age-depth function based on Southern Hemisphere calibration (McCormac et al., 2004) of six ^{14}C dates with the 2_ error displayed, the levels of the measured ^{10}Be samples, magnetic susceptibility (10^{-6} m^3 kg^{-1}), weight % of carbon (C) and nitrogen (N), the C/N ratio, and cumulative percentage curves for Polypodiaceae (fern) spores, Phylica arboreae (island-tree) pollen, and the sum of grass, sedge and herb pollen grains. The dashed lines prior to 950 AD and after 1400 AD (left panel) show the necessary sedimentation rates for obtaining the expected ^{10}Be fluxes.

Although it is difficult to completely overcome these problems, we think that much of the desirable preconditions are met within our profile between 950 and 1400 AD, and therefore measurements of ^{10}Be content were limited to this time period. Furthermore, the 900–1500 AD period is known for its highly variable solar activity/^{10}Be fluxes (Beer et al., 1988; Vonmoos et al., 2006). In conclusion, with the constant sedimentation rate and homogenous lithology (Fig. 2), this location ought to be a good setting for detecting changes in ^{10}Be fluxes, and could therefore show a potential imprint of the variable production rate in the atmosphere, although a slight delay of the surface run-off transported ^{10}Be may have to be taken into account. Based on these preconditions, we can expect that ^{10}Be in the sediments analysed was deposited both directly from the atmosphere, being attached to aerosols and deposited with precipitation (McHargue and Damon, 1991), and through a fairly stable surface run-off of mainly organic particles with attached ^{10}Be. Furthermore, the high sedimentation rate offers the possibility to obtain records with a fairly high temporal resolution, which is necessary to study solar activity changes on decadal to centennial time scales.

3. Methods

Methods for the proxy records displayed in Fig. 2 are described in Ljung et al. (2006). Radiocarbon dating was carried out by the AMS ^{14}C laboratories in Poznan and Lund, and ^{14}C ages were converted to calibrated ages using the program OxCal v3.10 (Bronk Ramsey, 1995, 2001) and the SHCal04 calibration data-set (McCormac et al., 2004). Construction of the age-depth function is described in Ljung et al. (2006).

The ^{10}Be concentration in the sediment samples was measured in Zurich by the accelerator mass spectrometer (AMS) of ETH/PSI, which allows measurements of very small amounts of ^{10}Be (10^7 atoms). In the following, we describe the steps that were necessary to remove unwanted sediment material, which is necessary to get a clean sample for AMS measurements. In such measurements, ^{10}Be/^{9}Be ratios rather than absolute ^{10}Be concentrations are determined. Therefore, a known quantity of stable ^{9}Be is added to the sample (in our case: 0.6 mg ^{9}Be is added to approximately 3 g of sediment). We added 1 ml H_2O_2 (30%), 5 ml H_2O and 4 ml HCl to the sample/carrier mixture and let the sediments dissolve over the night. This procedure dissolves the sediment almost completely and we can assume that also the ^{10}Be is completely dissolved and retained for further analysis. Insoluble parts are removed by centrifugation and the fluids are removed by evaporation. Since the dried sample could still contain metals, we added 2 ml HCl (32%) and 2 ml H_2O and put the sample for 4 h into the centrifuge. After another drying step, we dissolved the sample by adding 1 ml HCl (32%) and 1 ml

(HNO_3). Any insoluble part was removed by another centrifugation step and by filtering the sample (0.4 μm pore size). Adding NH_4OH allows us to precipitate the beryllium hydroxide. The beryllium hydroxide is then dissolved again by adding 5 ml NaOH (pH 14, which ensures that other metal hydroxides are not dissolved). After waiting for another night, we retained the solution and precipitate Be by adding HCl (pH 7–10). Another centrifugation step allowed us to concentrate the Be. After that we added 2–3 ml HCl (1 M) and treated the sample as described in Yiou et al. (1997).

The results are expressed in concentrations, atoms per dry gram of sediment. To estimate the annual flux of ^{10}Be (atoms/(cm^2 yr)) to the Hillpiece Bog basin, dry bulk densities and sedimentation rate were calculated on all levels analysed for ^{10}Be (Table 2).

4. Results and discussion

We performed 15 measurements of ^{10}Be concentrations (atoms g^{-1} dry weight) between 280 and 195 cm (Table 2, Fig. 2), corresponding to 800–1450 AD. Through the bulk density values and the sedimentation rate, the concentration values could be converted into annual flux values (Fig. 3). The mean flux value for the 15 samples is 19.7 ($\pm$6.7) $\times 10^6$ atoms cm^{-2} yr^{-1}. If we consider that the bog is ca 5% of the whole catchment, and if we assume that most (or all) of the ^{10}Be deposited (with precipitation) in the catchment ended up in the lake sediments, the total flux to the bog, or former pond, should be approximately 20 times larger than the average flux to the catchment area. This would imply a mean ^{10}Be deposition rate of ca 1.0 ($\pm$0.35) $\times 10^6$ atoms cm^{-2} yr^{-1}, which is in the same order of magnitude as what Monaghan et al. (1986) and Masarik and Beer (1999) have calculated as the mean global-average ^{10}Be production rate: 1.21 and 0.58 $\times 10^6$ atoms cm^{-2} yr^{-1}, respectively. However, due to local-regional and temporal differences, the production rate varies between latitudes and environmental/climatic settings, as well as between periods of variable solar activity and magnetic field strength. For example, with today's magnetic field strength and a solar activity of 550 MeV, Tristan da Cunha's latitude has an average ^{10}Be production rate of 0.7 $\times 10^6$ atoms cm^{-2} yr^{-1} (Masarik and Beer, 1999). In

Table 2
Table showing sample depths, their calculated age (Fig. 2) with a constant sedimentation rate of 0.13 cm yr^{-1}, dry weight, dry density, measured concentrations of ^{10}Be atoms per dry g sediment, measurement error, calculated ^{10}Be flux in the Hillpiece Bog sediments and calculated ^{10}Be flux to the catchment considering the fact that the bog basin constitutes 5% of total catchment area

Sample depth range (cm)	Age range (years AD)	Dry weight (g)	Dry density (g cm^{-3})	^{10}Be conc. (atoms g^{-1})	^{10}Be flux in the Hillpiece Bog (atoms cm^{-2} yr^{-1})	Mean ^{10}Be flux to the drainage area (atoms cm^{-2} yr^{-1})
191–198.2	1477–1424	0.4316	0.1207	8.98e+8	14.187e+6	0.7093e+6
				±8.35e+7	±1.32e+6	±6.60e+4
198.2–204	1424–1378	0.3496	0.1216	8.53e+8	13.56e+6	0.6778e+6
				±4.44e+7	±7.05e+5	±3.2e+4
205.9–209.4	1363–1337	0.2986	0.132	7.83e+8	13.52e+6	0.6761e+6
				±3.29e+7	±5.68e+5	±2.84e+4
209.4–210.5	1337–1328	0.3133	0.1759	9.22e+8	21.20e+6	1.0600e+6
				±7.01e+7	±1.61e+6	±8.06e+4
210.5–215	1328–1294	0.9817	0.1913	11.97e+8	29.94e+6	1.4971e+6
				±6.22e+7	±1.56e+6	±7.78e+4
215–223.1	1294–1233	0.3641	0.1501	9.45e+8	18.55e+6	0.9275e+6
				±5.29e+7	±1.04e+6	±5.19e+4
223.1–230	1233–1179	0.4003	0.1376	7.02e+8	12.63e+6	0.6315e+6
				±3.79e+7	±6.82e+5	±3.41e+4
230–236.9	1179–1127	0.3806	0.1303	8.2e+8	13.99e+6	0.6994e+6
				±3.53e+7	±6.02e+5	±3.01e+4
236.9–242.4	1127–1085	0.4691	0.1301	9.44e+8	16.07e+6	0.8036e+6
				±2.83e+7	±4.82e+5	±2.41e+4
242.4–249.3	1085–1032	0.393	0.1379	12.1e+8	21.84e+6	1.0918e+6
				±4.24+7	±7.64e+5	±3.82e+4
249.1–254.1	1032–996	0.3261	0.1361	13.54e+8	24.11e+6	1.2059e+6
				±4.06e+7	±7.23e+5	±3.62e+4
254.1–260.9	996–944	0.293	0.1372	9.96e+8	17.88e+6	0.8940e+6
				±6.67e+7	±1.20e+6	±5.99e+4
260.9–267.8	944–891	0.311	0.1362	10.91e+8	19.43e+6	0.9717e+6
				±7.53e7	±1.34e+6	±6.70+4
267.8–276.2	891–829	0.2911	0.1422	17.52e+8	32.61e+6	1.6303e+6
				±9.81e+7	±1.83e+6	±9.13e+4
276.2–283.4	829–775	0.351	0.1407	14.34e+8	26.41e+6	1.3204e+6
				±5.59e+7	±1.03e+6	±5.15e+4

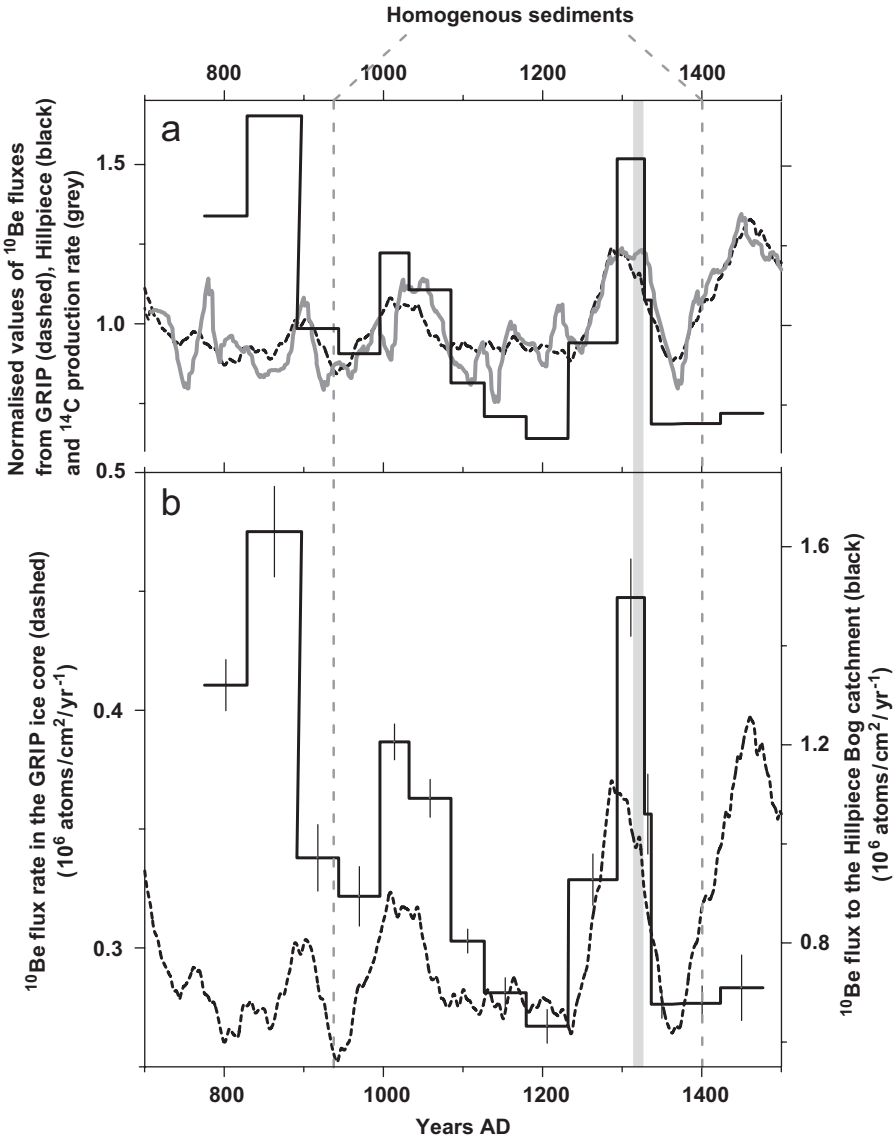

Fig. 3. (a) Comparison of normalised values of ^{10}Be measured in the sediments from Tristan da Cunha with independent estimates of the ^{10}Be and ^{14}C production rates. The 15 levels of ^{10}Be fluxes in Hillpiece Bog (black) are compared with a 50-yr running average of the ^{14}C production rate (grey) based on the tree-ring ^{14}C record (Reimer et al., 2004) and 50-yr smoothed ^{10}Be fluxes in the GRIP ice core (Muscheler et al., 2004; Vonmoos et al., 2006) (dashed) at Summit in Central Greenland. (b) The absolute ^{10}Be flux rates from the Hillpiece Bog catchment are compared with absolute flux rates from the GRIP ice core (Muscheler et al., 2004; Vonmoos et al., 2006). Measurement errors from the Hillpiece Bog samples are shown as vertical black lines. Note that the section with homogenous sediments is marked with vertical dashed lines, and the tephra-influenced sediment is shown as a grey bar. For calculations of the flux rates for the Hillpiece Bog catchment we refer to the text.

this context it should also be noted that topographic/orographic effects of, for example, an island significantly increases the precipitation, and thus also the ^{10}Be flux (Field et al., 2006). We therefore think that the Hillpiece Bog ^{10}Be flux record can be explained in terms of relatively direct ^{10}Be deposition from the atmosphere to the sediments. Therefore, during periods of stable environmental and sedimentary conditions, we think that the variations in ^{10}Be fluxes can be expected to reflect changes in the ^{10}Be production rate in the atmosphere.

To test this hypothesis, we present in Fig. 3 the calculated catchment flux rates, including measurement errors, compared with the ^{10}Be measurements in the GRIP ice core (Muscheler et al., 2004; Vonmoos et al., 2006). We also show the normalised values of these two rates compared to the normalised values of theoretical estimates of the ^{14}C production rate inferred from the tree-ring ^{14}C record (Muscheler et al., 2005) based on the INTCAL04 record (Reimer et al., 2004). Although the absolute values for the flux rates are lower in the GRIP ice core than our calculated values, the agreement in the general trends between 900 and 1400 AD is good ($r = 0.8$, $p < 0.05$). Our ^{10}Be record also harmonises well with the variations in the ^{14}C production rate regarding both timing and amplitude between 900 and 1400 AD ($r = 0.6$, $p < 0.05$). The radionuclide production peaks around 1000 and 1300 AD (Wolf

solar minimum) and the relative production rate changes concur between the two independent records, and the agreement between the records is hardly a matter of chance. This implies a common production-related cause for the observed variation, at least during the period of homogenous sedimentation (Fig. 3). Since high-resolution geomagnetic field records cannot explain such short-term ^{10}Be and ^{14}C production rate changes (Muscheler et al., 2007), these observed changes are most likely due to the variable solar shielding of galactic cosmic rays. We therefore think that we have detected solar-induced production rate changes in the sediments of the Hillpiece Bog.

The ^{10}Be fluxes of the 2–3 oldest samples (Fig. 3) are much higher than expected. This we relate to a different depositional and catchment environment before 950 AD, shown by the different lithology, magnetic susceptibility values and vegetation composition (Fig. 2). Lake catchment before this change was more open, shown by higher grass and herb pollen values, and the sediments have higher magnetic susceptibility values in spite of maximum values of organic C. These anomalously high flux values can have different causes, e.g. that sedimentation rates were lower before 950 AD than assumed by the age model in Fig. 2. Sedimentation rates necessary to explain the anomalous values are shown by the dashed line (Fig. 2) and are not unrealistic. With these rates, the time resolution would be low and details of ^{10}Be flux changes would be hard to detect. Another or additional reason for these anomalies could be that the more open landscape led to increased erosion of exposed organic soils. The latter explanation is supported by the several small susceptibility peaks at 280–260 cm (Fig. 2) possibly documenting the presence of fine-grained detrital magnetite, rich in ultra-fine grained superparamagnetic particles (Oldfield, 1994), formed through pedogenesis (Maher, 1998), to which ^{10}Be could attach. Increased erosion of more exposed organic soils may thus have been responsible for both the susceptibility peaks (Björck et al., 2000) and the high ^{10}Be fluxes.

Although our record displays the ^{10}Be peak at 1000 AD and the Wolf solar minimum at 1300 AD (Fig. 3), the effect of the Spoerer solar minimum at 1450 AD is not seen in our topmost sample. However, it is noteworthy that susceptibility increases and vegetation changes (Fig. 2) at 1400 AD, implying different sedimentary and environmental conditions compared to before. This anomaly with the lack of a ^{10}Be peak at 1450 AD can be explained by the inability to date the core in detail. The necessary increase in accumulation rate to account for the higher fluxes—see dashed line in Fig. 2—would also mean that the peak is situated further up in the sediment record, and that we would only see the rising values before the peak (Fig. 3). In the context of the discussion on solar activity and climate connections, one could, for example, also speculate if the low solar activity during the Spoerer minimum caused an increased precipitation at Tristan and thereby also increased accumulation rates.

The environmental and sedimentary changes at 900–950 AD and at 1450 AD demonstrate that a stable environment with homogenous sedimentation is required to obtain ^{10}Be records that can be interpreted in terms of production rate changes. In this context, it is interesting to note the susceptibility peak at 212–217 cm (Fig. 2). It is related to a 0.5 cm thin and distinct volcanic ash layer, and its broader response in susceptibility is possibly a result of heavier ash particles having sunk into the organic-rich sediment–water interface at the deposition. Its distinct character implies immediate atmospheric deposition at the eruption, but the marked ^{10}Be peak at that level (Fig. 3) may indicate additional particles—tephra—to which ^{10}Be was attached. However, as this peak coincides with distinct peaks in GRIP ^{10}Be fluxes and ^{14}C production rate (Fig. 3), it indicates that tephra fall-outs only seem to have a restricted influence on the ^{10}Be deposition.

We think that our study demonstrates the fact that solar variations can be reconstructed from sedimentary sequences by the use of ^{10}Be. With its half-life of 1.5 million years, this implies that solar activity and geomagnetic field changes can be reconstructed throughout at least the Quaternary period if suitable sediments are found. Combined with tree-ring ^{14}C data and ice core ^{10}Be measurements, such measurements have also the potential to improve the solar activity reconstructions during this period extending the range of ^{14}C data and ice core records. Finally, such measurements can give clues for the mechanisms and timing of the solar influence on climate, especially if ^{10}Be data and other climate proxies can be obtained from the same sediments.

Acknowledgements

Ole Bennike and Dan Hammarlund are acknowledged for help during field work, and Felicty and James Glass provided the logistics on Tristan da Cunha. Silvia Bolhander is thanked for preparing samples for ^{10}Be measurements. The study was financed by the Swedish Research Council (VR) by grants to SB's 'Atlantis' project, and by the Swiss National Science Foundation. Comments by two anonymous referees improved the final version of the paper.

References

Anderson, R.F., Lao, Y., Broecker, W.S., Trumbore, S.E., Hofmann, H.J., Wolfi, W., 1990. Boundary scavenging in the Pacific Ocean: a comparison of ^{10}Be and ^{231}Pa. Earth and Planetary Science Letters 96, 287–304.

Baker, P.E., Gass, I.G., Harris, P.G., Le Maitre, R.W., 1964. The volcanological report of the royal society expedition to Tristan da Cunha, 1962. Philosophical Transactions of the Royal Society of London, Series A, Mathematical and Physical Science 256, 439–575.

Beer, J., Siegenthaler, U., Bonani, G., Finkel, R.C., Oeschger, H., Suter, M., Wölfi, W., 1988. Information on past solar activity and geomagnetism from ^{10}Be in the Camp Century ice core. Nature 331, 675–679.

Beer, J., Blinov, A., Bonani, G., Finkel, R.C., Hofmann, H.J., Lehman, B., Oeschger, H., Sigg, A., Schwander, J., Staffelbach, T., Stauffer, B., Suter, M., Wölfi, W., 1990. Use of ^{10}Be in polar ice to trace the 11-year cycle of solar activity. Nature 347, 164–166.

Björck, S., Noe-Nygaard, N., Wolin, J., Houmark-Nielsen, M., Jorgen Hansen, H., Snowball, I., 2000. Eemian lake development, hydrology and climate: a multi-stratigraphic study of the Hollerup site in Denmark. Quaternary Science Reviews 19, 509–536.

Bronk Ramsey, C., 1995. Radiocarbon calibration and analysis of stratigraphy: the OxCal program. Radiocarbon 37, 425–430.

Bronk Ramsey, C., 2001. Development of the radiocarbon program OxCal. Radiocarbon 43, 381–389.

Chase, Z., Anderson, R.F., Fleisher, M.Q., Kubik, P.W., 2002. The influence of particle composition and particle flux on scavenging of Th, Pa and Be in the ocean. Earth and Planetary Science Letters 204, 215–229.

Christl, M., Strobl, C., Mangini, A., 2003. Beryllium-10 in deep-sea sediments: a tracer for the Earth's magnetic field intensity during the last 200,000 years. Quaternary Science Reviews 22, 725–739.

Field, C.V., Schmidt, G.A., Koch, D., Salyak, C., 2006. Modeling production and climate-related impacts on ^{10}Be concentration in ice cores. Journal of Geophysical Research 111, D15107.

Frank, M., Schwarz, B., Baumann, S., Kubik, P.W., Suter, M., Mangini, A., 1997. A 200 kyr record of cosmogenic radionuclide production rate and geomagnetic field intensity from ^{10}Be in globally stacked deep-sea sediments. Earth and Planetary Science Letters 149, 121.

Houriuchi, K., Minoura, K., Kobayashi, K., Nakamura, T., Hatori, S., Matsuzaki, H., Kawai, T., 1999. Later-glacial to post-glacial ^{10}Be fluctuations in a sediment core from the Academician Ridge, Lake Baikal. Geophysical Research Letters 26, 1047–1050.

Lal, D., Peters, B., 1967. Cosmic ray produced radioactivity on the Earth. In: Flügge, S. (Ed.), Hanbuch der Physik. Springer, Berlin, pp. 551–612.

Libby, W.F., 1955. Radiocarbon dating. Chicago University Press, Chicago.

Ljung, K., Björck, S., Hammarlund, D., Barnekow, L., 2006. Late Holocene multi-proxy records of environmental change on the South Atlantic island Tristan da Cunha. Palaeogeography, Palaeoclimatology, Palaeoecology 241, 539–560.

Maher, B.A., 1998. Magnetic properties of modern soils and Quaternary loessic paleosols: paleoclimatic implications. Palaeogeography, Palaeoclimatology, Palaeoecology 137, 25–54.

Masarik, J., Beer, J., 1999. Simulation of particle fluxes and cosmogenic nuclide production in the Earth's atmosphere. Journal of Geophysical Research 104, 12,099–12,111.

McCormac, F.G., Hogg, A.G., Blackwell, P.G., Buck, C.E., Higham, T.F.G., Reimer, P.J., 2004. SHCal04 Southern Hemisphere calibration, 0–11 kyr cal BP. Radiocarbon 46, 1087–1092.

McHargue, L.R., Damon, P.E., 1991. The global beryllium 10 cycle. Review of Geophysics 29, 141–158.

Monaghan, M.C., Krishnaswami, S., Turekian, K.K., 1986. The global-average production rate of ^{10}Be. Earth and Planetary Science Letters 76, 279–287.

Muscheler, R., Beer, J., Wagner, G., Laj, C., Kissel, C., Raisbeck, G.M., Yiou, F., Kubik, P.W., 2004. Changes in the carbon cycle during the last deglaciation as indicated by the comparison of ^{10}Be and ^{14}C records. Earth and Planetary Science Letters 219, 325–340.

Muscheler, R., Beer, J., Kubik, P.W., Synal, H.A., 2005. Geomagnetic field intensity during the last 60,000 years based on ^{10}Be and ^{36}Cl from the Summit ice cores and ^{14}C. Quaternary Science Reviews 24, 1849–1860.

Muscheler, R., Joos, R., Beer, J., Mueller, S.A., Vonmoos, M., Snowball, I., 2007. Solar activity during the last 1000 years inferred from radionuclide records. Quaternary Science Reviews 26, 82–97.

Oldfield, F., 1994. Towards the discrimination of fine grained ferrimagnets by magnetic measurements in lake and near-shore marine sediments. Journal of Geophysical Research 99, 9045–9050.

Reimer, P.J., Baillie, M.G.L., Bard, E., Bayliss, A., Beck, J.W., Bertrand, C.J.H., Blackwell, P.G., Buck, C.E., Burr, G.S., Cutler, K.B., Damon, P.E., Edwards, R.L., Fairbanks, R.G., Friedrich, M., Guilderson, T.P., Hogg, A.G., Hughen, K.A., Kromer, B., McCormac, G., Manning, S., Ramsey, C.B., Reimer, R.W., Remmele, S., Southon, J.R., Stuiver, M., Talamo, S., Taylor, F.W., van der Plicht, J., Weyhenmeyer, C.E., 2004. IntCal04 terrestrial radiocarbon age calibration, 0–26 cal kyr BP. Radiocarbon 46, 1029–1058.

Siegenthaler, U., Heimann, M., Oeschger, H., 1980. ^{14}C variations caused by changes in the global carbon cycle. Radiocarbon 22, 177–191.

Van Geel, B., Mook, W.G., 1989. High-resolution ^{14}C dating of organic deposits using natural atmospheric ^{14}C variations. Radiocarbon 31, 151–156.

Vonmoos, M., Beer, J., Muscheler, R., 2006. Large variations in Holocene solar activity: constraints from ^{10}Be in the Greenland Ice Core Project ice core. Journal of Geophysical Research 111, A10105.

Yiou, F., Raisbeck, G.M., Baumgartner, S., Beer, J., Hammer, C., Johnsen, S., Jouzel, J., Kubik, P.W., Lestringuez, J., Stiévenard, M., Suter, M., Yiou, P., 1997. Beryllium 10 in the Greenland Ice Core Project ice core at Summit, Greenland. Journal of Geophysical Research 102, 26783–26794.